Possible magnetic ground state in the perovskite $SrCoO_3$

Min Zhuang, Weiyi Zhang, An Hu, and Naiben Ming
National Laboratory of Solid State Microstructures and Department of Physics, Nanjing University, Nanjing 210093, China
(Received 9 December 1997; revised manuscript received 16 January 1998)

The magnetic ground state of cobalt perovskite $SrCoO_3$ is under much debate at present due to its complex magnetic properties. To shed further light on this issue we have studied various magnetic structures of enlarged double cells. The calculation is carried out self-consistently within the unrestricted Hartree-Fock approximation and the real-space recursion method. Our results show that the magnetic ground state mainly depends on the competition between the crystal field strength Dq and Hund's coupling j. For a fixed j, it can be either the intermediate-spin state ($t_{2g}^4e_g^1$), the low-spin–intermediate-spin ferromagnetically and charge-ordered state ($t_{2g}^5e_g^0$-$t_{2g}^4e_g^1$-FM), or the low-spin state ($t_{2g}^5e_g^0$) as Dq increases. However, the intermediate-spin state is the most probable candidate for the magnetic ground state in view of the experimental photoemission spectra and magnetic moment. [S0163-1829(98)00322-1]

I. INTRODUCTION

The magnetic perovskite compounds have attracted much attention in the past few years due to their very interesting physical properties. Colossal magnetoresistance was observed in doped $La_{1-x}Sr_xMnO_3$ (Ref. 1) and various possible mechanisms were proposed. The finite-temperature transition at 90 K in $LaCoO_3$ is another hotly discussed issue.[2–4] While it is generally agreed that the low-temperature phase is a nonmagnetic low-spin state ($t_{2g}^6e_g^0$), both the high-spin state[2–7] ($t_{2g}^4e_g^2$) and intermediate-spin state[8,10] ($t_{2g}^5e_g^1$) were proposed for the high-temperature phase. Recently, fairly large magnetoresistance was also observed in the doped cobalt perovskite $La_{1-x}A_xCoO_3$ (A=Ca, Sr, or Ba) (Ref. 11) and the magnetic phase diagram as a function of doping was determined.[12]

The magnetic state of doped $La_{1-x}A_xCoO_3$ strongly depends on the doping concentration x. While the undoped compound is a nonmagnetic insulator, the system takes the spin-glass state for low doping concentration $0<x<0.18$ (Refs. 5 and 12) and the ferromagnetic state for higher doping concentration $0.18<x<\leqslant 1.0$.[12–14] The doping also changes the valence of Co ions. The compound becomes a mixed valence system with both Co^{+3} and Co^{+4}. Previously, the magnetic state of doped $La_{1-x}A_xCoO_3$ was suggested to be a mixture of the high-spin Co^{+3}($t_{2g}^4e_g^2$) and the low-spin Co^{+4}($t_{2g}^5e_g^0$) ions[13] because the measured saturation magnetic moment is only about half of the moment of the high-spin Co^{+3} ions.[13–14] More recently, the Sr-induced intermediate-spin state was also proposed for the doped state based on the photoemission spectra[15] and the ferromagnetic resonance experiment.[16] The comparison between the experimental Co $2p$ x-ray-absorption spectra and the atomic multiplet calculation also indicated that the ground state of $SrCoO_3$ is the intermediate-spin state ($t_{2g}^4e_g^1$).[17]

In order to better understand the magnetic properties of the doped system, it is worthwhile to first study the simpler end member compound $SrCoO_3$. Once a clear picture is obtained for the magnetic structure in perovskite $SrCoO_3$, it certainly will help us to resolve the complex situation in the doped perovskite. Thus we study, in this paper, various magnetic states in an enlarged double cell of $SrCoO_3$. In addition to the low-spin (LS) state ($t_{2g}^5e_g^0$), intermediate-spin (IS) state ($t_{2g}^4e_g^1$), and high-spin (HS) state ($t_{2g}^3e_g^2$), we also consider all possible spin and charge ordered combinations among the three states. Note that the definitions of these three states are different from the ones in the other end member $LaCoO_3$ because the former has one electron less than the latter. The calculation is performed within the unrestricted Hartree-Fock approximation on a realistic perovskite-type lattice model and the self-consistent solutions are obtained using the iteration method. To compare the relative stability of the various states, we compute their energies as functions of the crystal-field strength $10Dq$ and Hund's coupling j since the phase diagram mainly depends on the competition between these two parameters. Our results show that for a fixed Hund coupling j, the ground state of the system changes from the IS state to the LS-IS ferromagnetic (FM) and charge ordered state and finally to the LS state as Dq increases. According to the parameters typical for cobaltites and the experimental magnetic moment,[13] we suggest that the ground state of $SrCoO_3$ is in the intermediate-spin state regime, which is in agreement with the results of the Co $2p$ x-ray-absorption spectroscopy spectrum.[17]

The rest of the paper is organized as follows. In Sec. II we first introduce the perovskite-type lattice model and the unrestricted Hartree-Fock approximation and then the real space recursion method is also briefly outlined. In Sec. III we present the numerical results and the corresponding discussion for each state. In particular, we pay special attention to the stability of various states and propose the most probable candidate for the ground state of this compound. The conclusion is drawn in Sec. IV.

II. THEORETICAL FORMULISM

We adopt the multiband d-p model Hamiltonian[9] to describe such transition metal oxides, which includes the full degeneracy of the transition metal $3d$ orbitals and oxygen $2p$ orbitals as well as on-site Coulomb and exchange interactions:

$$\mathcal{H}=\sum_{i,m,\sigma}\epsilon^0_{dm}d^\dagger_{im\sigma}d_{im\sigma}+\sum_{j,n,\sigma}\epsilon_p p^\dagger_{jn\sigma}p_{jn\sigma}+\sum_{i,j,m,n,\sigma}(t^{mn}_{ij}d^\dagger_{im\sigma}p_{jn\sigma}+\text{H.c.})+\sum_{i,j,n,n',\sigma}(t^{nn'}_{ij}p^\dagger_{in\sigma}p_{jn'\sigma}+\text{H.c.})+\sum_{i,m}ud^\dagger_{im\uparrow}d_{im\uparrow}d^\dagger_{im\downarrow}d_{im\downarrow}+\frac{1}{2}\sum_{i,m,\neq,m',\sigma,\sigma'}\tilde{u}d^\dagger_{im\sigma}d_{im\sigma}d^\dagger_{im'\sigma'}d_{im'\sigma'}-j\times\sum_{i,m,\sigma,\sigma'}d^\dagger_{im\sigma}\boldsymbol{\sigma}d_{im\sigma'}\cdot\mathbf{S}^d_{im}, \quad (1)$$

where $d_{im\sigma}$ ($d^\dagger_{im\sigma}$) and $p_{jn\sigma}$ ($p^\dagger_{jn\sigma}$) denote the annihilation (creation) operators of an electron on Co d at site i and O p at site j, respectively, and ϵ^0_{dm} and ϵ_p are their corresponding on-site energies. m and n refer to the orbital index and σ to the spin. The crystal-field-splitting energy is included in ϵ^0_{dm}, i.e., $\epsilon^0_d(t_{2g})=\epsilon^0_d-4Dq$ and $\epsilon^0_d(e_g)=\epsilon^0_d+6Dq$, where ϵ^0_d is the bare on-site energy of the d orbital. t^{mn}_{ij} and $t^{nn'}_{ij}$ are the nearest neighbor hopping integrals for p-d and p-p, which are expressed in terms of Slater-Koster parameters $(pd\sigma)$, $(pd\pi)$, $(pp\sigma)$, and $(pp\pi)$.[18] $\mathbf{S}^d_{im}$ is the total spin operator of the Co ion extracting the spin-operator in orbital m, $\tilde{u}=u-5j/2$. The parameter u is related to the multiplet averaged d-d Coulomb interaction U via $u=U-(20/9)j$.

In the unrestricted Hartree-Fock approximation, the Hamiltonian becomes linearized and is reduced to

$$\mathcal{H}=\sum_{i,m,\sigma}\left[\epsilon^0_{dm}+un^d_{im\bar{\sigma}}-\frac{j}{2}\sigma(\mu^d_t-\mu^d_m)+\tilde{u}(n^d_t-n^d_m)\right]\times d^\dagger_{im\sigma}d_{im\sigma}+\sum_{j,n,\sigma}\epsilon_p p^\dagger_{jn\sigma}p_{jn\sigma}+\sum_{i,j,m,n,\sigma}(t^{mn}_{ij}d^\dagger_{im\sigma}p_{jn\sigma}+\text{H.c.})+\sum_{i,j,n,n',\sigma}(t^{nn'}_{ij}p^\dagger_{in\sigma}p_{jn'\sigma}+\text{H.c.}). \quad (2)$$

Here $n^d_{m\sigma}=\langle d^\dagger_{m\sigma}d_{m\sigma}\rangle$, $\mu^d_m=n^d_{m\uparrow}-n^d_{m\downarrow}$, and n^d_t and μ^d_t are the total electron numbers and magnetization of the Co d orbitals. We have chosen the z axis as the spin quantization axis.

For the tight-binding Hamiltonian (2), the density of states can be easily calculated using the real space recursion method.[19] Instead of diagonalizing the Hamiltonian with the dimension of the number of orbitals in the primitive cell, the recursion methods choose one particular lattice site, where the density of states is acquired, and tridiagonalizes the Hamiltonian to a certain number of levels; one then writes the Green's function as

$$G(\omega)=\cfrac{b_0^2}{\omega-a_0-\cfrac{b_1^2}{\omega-a_1-\cfrac{b_2^2}{\omega-a_2-\cfrac{b_3^2}{\omega-a_3-\cdots}}}}. \quad (3)$$

The coefficients a_i and b_i are obtained from the tridiagonalization of the tight-binding Hamiltonian matrix for a given starting orbital. The multiband terminator[20] is chosen in our calculation to close the continuous fractional. To study the modulated spin states in $SrCoO_3$, we have considered various spin and charge ordered states of an enlarged double cell of $SrCoO_3$. This is achieved by taking the different initial values of the electron number and magnetic moment for different lattice sites and orbitals. There are 38 orbitals to be calculated for each iteration and we compute 25 levels for the continuous fractional coefficients for each orbital. We have checked our results for different levels to ensure the accuracy of energy calculation and better than 5 meV in energy accuracy is secured. The whole procedure is iterated self-consistently untill convergence and the density of states is obtained by $\rho_{m\sigma}(\omega)=-(1/\pi)\text{Im}G_{m\sigma}(\omega)$. This allows us to calculate the electron numbers, magnetic moments, and the energies of various ordered states.

III. NUMERICAL RESULTS AND DISCUSSION

Although the direct parameters of $SrCoO_3$ is not available, their values can be inferred from those of $LaCoO_3$ since they mainly differ from each other on the number of valence electrons in the unit cell. Thus, on the assumption that doping does not affect the intrinsic parameters of the cobalt oxide, the bare on-site energies of Co d and O p orbitals are taken as $\epsilon^0_d=-28.0$ eV and $\epsilon_p=0$ eV. The Slater-Koster parameters are $(pd\sigma)=-2.0$ eV, $(pd\pi)=0.922$ eV, $(pp\sigma)=0.6$ eV, and $(pp\pi)=-0.15$ eV, respectively. The on-site Coulomb repulsion is $U=5.0$ eV. The crystal field strength and Hund's coupling are set as $Dq=0.16$ eV and $j=0.84$ eV. With the parameter set given above, we have studied the electronic structures of various spin and charge ordered states and ten different structures are found to be metastable.

In Figs. 1(a) and 1(b), we present the spin resolved total densities of states of the double cell for the low-spin state ($t^5_{2g}e^0_g$, $S=1/2$) and the intermediate-spin state ($t^4_{2g}e^1_g$, $S=3/2$). The solid and dotted lines denote the density of states of the majority spin and minority spin, respectively. The high-spin state ($t^3_{2g}e^2_g$, $S=5/2$) turns out to be unconvergent due to the strong superexchange interaction.[17] The low-spin state is a metallic state with a low density of states at the Fermi energy. The peaks near the Fermi energy come from t_{2g} electrons and the main body of the valence band is derived mostly from O p orbitals. The metallic nature of $SrCoO_3$ is due to the fact that it has one electron less than $LaCoO_3$; one of the bands is only half filled. The intermediate-spin state is also a metallic state; it has a broader bandwidth than that of the low-spin state. Surprisingly, the density of states just below the Fermi energy in the valence band is mainly of O p character and the contribution of t_{2g} electrons shifts to the lower-energy region around -7 eV; the whole spectrum has less structure than the nonmagnetic ground state of $LaCoO_3$. These features are in agreement with the experimental observations that the photoemission spectrum becomes smooth and the density of states near the Fermi energy is more and more of O p character[15] as the system is doped. The intermediate-spin state also has the right magnetic moment $2.96\mu_B$, which is

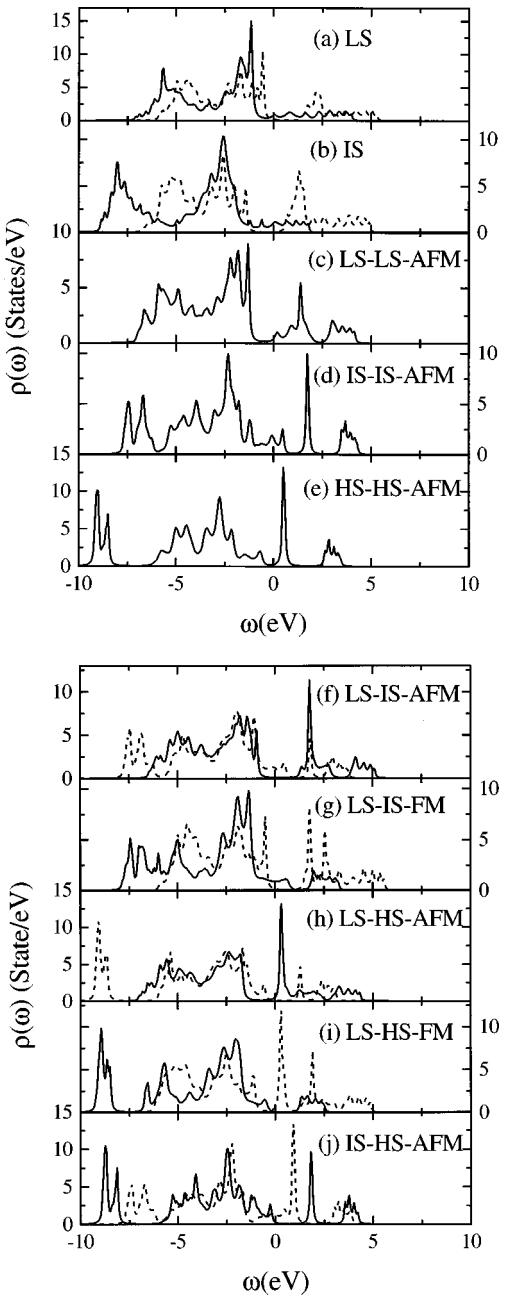

FIG. 1. Spin resolved total density of states for ten different spin and charge ordered structures at $j=0.84$ eV and $Dq=0.16$ eV. The other parameters are described in the text. The solid line and dotted line refer to the density of states for the majority spin and minority spin, respectively.

close to the experimental value $3.0\mu_B$.[13] Later we will show that the intermediate-spin state has the lowest energy in the relevant parameter regime among all the structures studied.

Next we investigate the nearest-neighbor antiferromagnetically ordered structures LS-LS-antiferromagnetic (AFM), IS-IS-AFM, and HS-HS-AFM states. This was done in an enlarged double cell and the total density of states are shown in Figs 1(c)–1(e). The majority-spin and minority-spin total densities of states are the same because the two Co ions have the opposite magnetic moment. In the LS-LS-AFM state, the gross structure is similar to the one of the LS state except that a gap appears around the Fermi energy, whose size increases with Dq; the energy of the LS-LS-AFM state is also close to that of the LS-LS-FM state. The density of states of the IS-IS-AFM state has more structures than that of IS state due to the long-range antiferromagnetic ordering. Furthermore, the IS-IS-AFM state is a metal with a relatively high density of states at the Fermi energy. As can be seen in Fig. 1(e), the HS-HS-AFM state has the broadest bandwidth, probably due to its largest magnetic moment; it corresponds to a semiconductor as a gap exists at the Fermi energy.

In addition to the above spin structures, we have studied various spin and charge ordered structures among different spin states of neighboring Co ions. This is achieved by taking into account the different initial values of the electron number and magnetic moment for the neighboring lattice sites and orbitals. The first two structures are the LS-IS-AFM state and the LS-IS-FM state where the neighboring LS and IS moments align antiferromagnetically and ferromagnetically, respectively. The spin resolved total density of states, as shown in Figs. 1(f) and 1(g) suggests that these two structures have a similar spectral shape for the small magnetic moment of the LS Co ion. In particular, the moment of the LS Co ion in the LS-IS-AFM state is $0.66\mu_B$, which is smaller than $1.58\mu_B$ in the LS-IS-FM state, while the moment of the IS Co ion has almost the same value in these two states.

Similar structures can be obtained by substituting the spin state of the Co ion. They are the LS-HS-AFM, LS-HS-FM, and IS-HS-AFM structures and their spin resolved total densities of states are shown in Figs. 1(h)–1(j). Just like the HS-HS-FM structure, the IS-HS-FM does not converge due to the large superexchange interaction. The shape of the spectra of the spin resolved total density of the states of LS-HS-AFM and LS-HS-FM structures is similar to those shown in Figs. 1(h) and 1(i). The pseudogaps at the Fermi energy in these two structures become enhanced as Dq decreases. In Fig. 1(j), the density of state of the IS-HS-AFM state is shown. The complex structures are caused by the larger magnetic moment as well as the long-range antiferromagnetic order. The electron numbers, magnetic moments of the Co d band, and energy are summarized in Table I for all the spin and charge ordered structures. One sees that the IS state has the lowest energy and thus is the ground state.

The results for the various A-type AFM states among different spin states of the Co ion are not presented here because they never become the absolute ground state in the parameter range we studied due to the lack of the Jahn-Teller effect in the $SrCoO_3$ compound. In fact, our calculation shows that the energy of these states always lies between the corresponding G-type AFM states and FM states. This conclusion is similar to the case of cubic $LaMnO_3$ when the Jahn-Teller effect is neglected.[21] The A-type AFM state becomes the ground state only when the Jahn-Teller effect is strong, which is not the case for $SrCoO_3$.

In all the magnetic structures studied above, there is a common feature in the density of states. The peaks in all the spectra come mainly from t_{2g} electrons, which indicates that t_{2g} electrons are easily localized. The flat e_g band is responsible for the itinerant behavior of the system, which is similar to the Mn perovskite. Since Sr doping induces a transition from a nonmagnetic insulator to a ferromagnetic metal, it implies that $La_{1-x}Sr_xCoO_3$ is also a double exchange system.[22] However, no significant Jahn-Teller effect is ob-

TABLE I. Occupancy n^d and magnetic moment μ^d/μ_B of Co ions in the double cell of various structures at $Dq=0.16$ eV and $j=0.84$ eV.

Structure type	n_1^d	μ_1^d	n_2^d	μ_2^d	Energy
LS	6.48	1.28	6.48	1.28	−212.544
IS	6.33	2.96	6.33	2.96	−212.911
LS-LS-AFM	6.46	1.09	6.46	−1.09	−212.475
IS-IS-AFM	6.38	2.73	6.38	−2.73	−212.103
HS-HS-AFM	6.49	3.73	6.49	−3.73	−211.620
LS-IS-FM	6.56	1.58	6.31	2.89	−212.841
LS-IS-AFM	6.52	0.66	6.32	−2.96	−212.548
LS-HS-FM	6.55	1.57	6.10	3.70	−212.485
LS-HS-AFM	6.52	0.65	6.09	−3.78	−212.184
IS-HS-AFM	6.40	2.77	6.14	−3.75	−211.900

served in the cobaltites. The magnetoresistance in the doped $LaCoO_3$ can be described by the so-called double exchange mechanism, which makes for an interesting comparison with the doped $LaMnO_3$. From Table I we find that the occupancy of the d band is always larger than 6, coinciding with the fact that $SrCoO_3$ has a considerable amount of the ligand hole character. The Co moment is approximately unchanged in all the structures except that the LS Co ion in the LS-IS-AFM structure and LS-HS-AFM structure has a smaller moment than that of the corresponding ferromagnetic states.

It is of interest to compare the relative stability of all the structures discussed above to obtain the ground state of $SrCoO_3$. In Fig. 2 we have calculated energies of various spin structures as a function of the crystal field strength Dq for a fixed Hund coupling $j=0.84$ eV. Dq changes from 0.10 eV to 0.22 eV. For weak crystal field strength, the IS state is the ground state of the system; as Dq increases to 0.172 eV, the LS-IS-FM state becomes energetically more favorable; the LS state becomes the stable state when Dq approaches 0.197 eV. Other structures we studied are energetically unfavorable in the relevant parameter region of the compound. Since Hund's coupling j and the crystal field strength Dq affect the energies in a correlated fashion, we have checked our results for different j's. Our calculation found that the crossover point from IS to LS-IS-FM structures takes the values $Dq=0.156$, 0.172, and 0.186 eV for $j=0.80$, 0.84, and 0.88 eV, respectively. Similarly, the crossover point from LS-IS-FM to LS structures takes the values $Dq=0.184$, 0.197, and 0.212 eV at the same j's. Thus the crystal field strength Dq compensates the effect of Hund's coupling and the crossover point Dq increases with j. Note that the region of stability for the LS-IS-FM structure is almost independent of j.

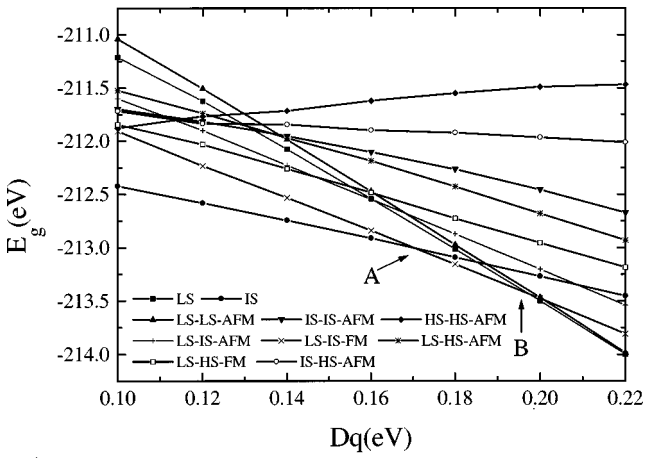

FIG. 2. Energies of the various spin and charge ordered structures as a function of Dq for $j=0.84$ eV. A and B indicate the crossover points for the transitions from the IS state to the LS-IS-FM state and the LS-IS-FM state to the LS state, respectively. Other parameters are the same as in Fig. 1.

Based on the energies of various structures and comparing the calculated density of states and magnetic moment with the experimental spectroscopy and measured moment, the IS state is the most suitable candidate for the ground state of $SrCoO_3$ in the relevant parameter region of the compound. Its density of states has the correct oxygen character below the Fermi energy and it has the right magnetic moment. In addition, the Sr doping induces a transition from a nonmagnetic insulator to an intermediate-spin ferromagnetically ordered structure is also consistent with the experimental observations.[13–17] Thus we discuss below the intermediate-spin state in more detail.

In Fig. 3 we present the spin resolved partial densities of states. The upper panel shows the densities of states of Co t_{2g} and Co e_g orbitals and the lower panel shows those of O p orbitals. The majority-spin density of states is plotted upward and the minority-spin density of states is plotted downward. One sees from this figure that the density of states of the Co t_{2g} orbital is very localized and that of Co e_g orbital is quite extended. The O p orbital forms the broader valence band just below the Fermi energy, which is consistent with the O p character observed in the photoemission spectra. Another interesting feature of the density of states is the half-metallic nature of the electronic structure as emphasized by Pickett and Singh.[21] The majority band has metallic character, while the minority band has band insulator character. The half-metallic property of the intermediate-spin state is most clearly seen from its band structure as shown in Fig. 4. There are bands crossing the Fermi energy in the majority-spin band structure due to the mixing of Co e_g and O p orbitals, while the Fermi energy lies in the band gap in the minority-spin band structure.

IV. CONCLUSION

In summary, we have studied the various spin and charge ordered structures in an enlarged double cell of $SrCoO_3$. Ten

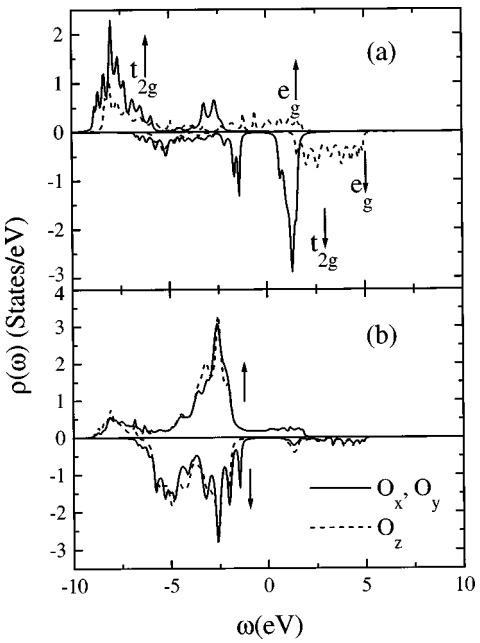

FIG. 3. Spin and orbital resolved partial density of states for the intermediate-spin state. The upper panel refers to the Co *d* orbital and the lower panel refers to the O *p* orbital. The parameters are the same as in Fig. 1.

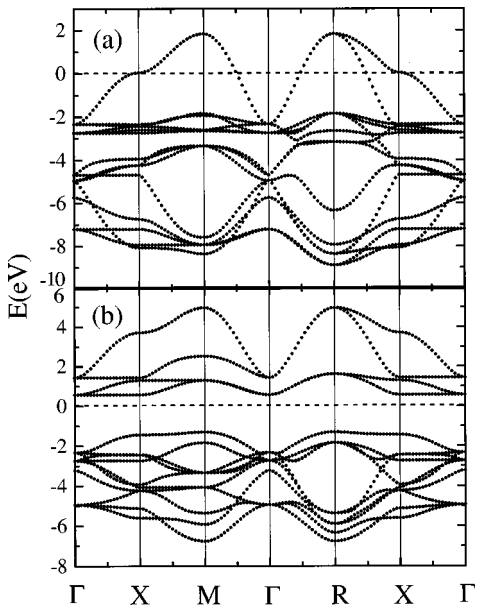

FIG. 4. Spin resolved band structure of the intermediate-spin state. The upper panel refers to the bands for the majority spin and the lower panel to the bands of the minority spin. The parameters are the same as in Fig. 1.

different structures are analyzed in details, using the unrestricted Hartree-Fock approximation of the multiband *d-p* model and the energy diagrams are obtained as functions of the crystal field strength and Hund's coupling. We find that the strong ligand hole character of the spectra suggests that the IS state is the ground state in the $SrCoO_3$ compound.

ACKNOWLEDGMENTS

This work was supported in part by the National Natural Science Foundation of China under Grants Nos. NNSF 19677202 and 19674027 and the key research project in the ''Climbing Program'' by the National Science and Technology Commission of China.

[1] See, for example, M. McCormack, S. Jin, T. H. Tiefl, R. M. Fleming, J. M. Phillips, and R. Ramesh, Appl. Phys. Lett. **64**, 3045 (1994); R. von Helmolt, J. Wecker, B. Holzapfel, L. Schultz, and K. Samwer, Phys. Rev. Lett. **71**, 2331 (1993).

[2] R. R. Heikes, R. C. Miller, and R. Mazelsky, Physica (Amsterdam) **30**, 1600 (1964).

[3] G. H. Jonker, J. Appl. Phys. **37**, 1424 (1966).

[4] P. M. Raccah and J. B. Goodenough, Phys. Rev. **155**, 932 (1967).

[5] K. Asai, O. Yokokura, N. Nishimori, H. Chou, J. M. Tranquada, G. Shirane, S. Higuchi, Y. Okajima, and K. Kohn, Phys. Rev. B **50**, 3025 (1994).

[6] M. Abbate, J. C. Fuggle, A. Fujimori, L. H. Tjeng, C. T. Chen, R. Potze, G. A. Sawatzky, H. Eisaki, and S. Uchide, Phys. Rev. B **47**, 16 124 (1993).

[7] S. R. Barman and D. D. Sarma, Phys. Rev. B **49**, 13 979 (1994).

[8] M. A. Korotin, S. Yu. Ezhov, I. V. Solovyev, V. I. Anisimov, D. I. Khomskii, and G. A. Sawatzky, Phys. Rev. B **54**, 5309 (1996).

[9] T. Mizokawa and A. Fujimori, Phys. Rev. B **54**, 5368 (1996).

[10] T. Saitoh, T. Mizokawa, A. Fujimori, M. Abbate, Y. Takeda, and M. Takano, Phys. Rev. B **55**, 4257 (1997).

[11] G. Briceno, X. D. Xiang, H. Chang, X. Sun, and P. G. Schultz, Science **270**, 273 (1995).

[12] M. Itoh, I. Natori, S. Kubota, and K. Motoya, J. Phys. Soc. Jpn. **63**, 1486 (1994).

[13] H. Taguchi, M. Shimada, and M. Koizumi, Mater. Res. Bull. **13**, 1225 (1978).

[14] G. H. Jonker and J. H. van Santen, Physica (Amsterdam) **19**, 120 (1953).

[15] T. Saitoh, T. Mizokawa, A. Fujimori, M. Abbate, Y. Takeda, and M. Takano, Phys. Rev. B **56**, 1290 (1997).

[16] D. Bahadur, S. Kollali, C. N. R. Rao, M. J. Patni, and C. M. Srivastava, J. Phys. Chem. Solids **40**, 981 (1979).

[17] R. H. Potze, G. A. Sawatzky, and M. Abbate, Phys. Rev. B **51**, 11 501 (1995).

[18] J. C. Slater and G. F. Koster, Phys. Rev. **94**, 1498 (1954).

[19] V. Heine, R. Haydock, and M. J. Kelly, in *Solid State Physics: Advances in Research and Applications*, edited by H. Ehrenreich, F. Seitz, and D. Turnbull (Academic, New York, 1980), Vol. 35, p. 215.

[20] R. Haydock and C. M. M. Nex, J. Phys. C **17**, 4783 (1984).

[21] W. E. Pickett and D. J. Singh, Phys. Rev. B **53**, 1146 (1996).

[22] C. Zener, Phys. Rev. **81**, 440 (1951).